Ceramics International xxx (xxxx) xxx–xxx

Contents lists available at ScienceDirect

Ceramics International

journal homepage: www.elsevier.com/locate/ceramint

Microwave dielectric properties of $Mg_4Nb_2O_9$-based ceramics with $(B_xW_{1-x})^{5+}$ substitutions at Nb^{5+} sites (B = Li, Mg, Al, Ti)

Jeong Hoon Kim, Eung Soo Kim*

Department of Materials Engineering, Kyonggi University, Suwon 443-760, Republic of Korea

ARTICLE INFO

Keywords:
Bond valence
Dielectric properties
Octahedral distortion

ABSTRACT

The dependences of the microwave dielectric properties on the isovalent substitution of $(Li^{1+}_{1/5}W^{6+}_{4/5})^{5+}$, $(Mg^{2+}_{1/4}W^{6+}_{3/4})^{5+}$, $(Al^{3+}_{1/3}W^{6+}_{2/3})^{5+}$ and $(Ti^{4+}_{1/2}W^{6+}_{1/2})^{5+}$ at the Nb^{5+}-sites of $Mg_4Nb_2O_9$ ceramics were investigated. For the samples sintered at 1350 °C for 10 h, a single phase of corundum structure with hexagonal symmetry was observed through the entire range of compositions. The structural characteristics of the $Mg_4Nb_{1.95}(B_xW_{1-x})_{0.05}O_9$ ceramics were quantitatively evaluated by Rietveld refinement method from the X-ray diffraction data. The specimens containing $(Ti^{4+}_{1/2}W^{6+}_{1/2})^{5+}$ substitutions had the highest quality factor (*Qf*) of 233,000 GHz of all the samples. The dielectric constants (*K*) of the samples were similar for all compositions. The temperature coefficient of the resonant frequency (*TCF*) of the samples was dependent on the distortion of the oxygen octahedra ($\Delta_{avg} \times 10^3$). As the distortion of the oxygen octahedra increased, the *TCF* values decreased and eventually become negative.

1. Introduction

The operating frequencies used for mobile communication are being continuously expanded in preparation for next-generation (5G) communication systems. Consequently, the microwave dielectric properties of materials such as the dielectric constant (*K*), the quality factor (*Qf*), and the temperature coefficient of resonant frequency (*TCF*) are more important than ever. Microwave dielectric ceramics should have a low *K* for fast signal transmission, a high *Qf* value to improve the resonant frequency selectivity, and a *TCF* of almost zero to enhance the thermal stability of the frequency [1].

In recent years, high *Qf* dielectric ceramics, such as ilmenite and corundum [2–4], have been investigated to improve the *Qf* further. According to previous reports [4] based on an understanding of the relationship between the structural characteristics and the microwave dielectric properties, the substitution of isovalent cations (for example, $(Li^{1+}_{1/4}Ta^{5+}_{3/4})^{4+}$, $(Mg^{2+}_{1/3}Ta^{5+}_{2/3})^{4+}$, and $(Al^{3+}_{1/2}Ta^{5+}_{1/2})^{4+}$) at the Ti-sites of $MgTiO_3$ ceramics with the ilmenite structure improves the microwave dielectric properties of these materials efficiently. For $MgTiO_3$ with the ilmenite structure, these isovalent substitutions, as well as tetravalent cation substitutions, at the Ti-sites improve the *Qf* value. This improvement may result from the differences in bonding between the cation and oxygen ions in the oxygen octahedra. In addition, because the corundum structure is an ordered derivative of the ilmenite structure, the microwave dielectric properties of materials with the corundum structure can be expected to be improved by isovalent substitution at its cation sites.

Typically, $Mg_4Nb_2O_9$ ceramics sintered at 1350 °C for 10 h have a *K* of 14, *Qf* of 210,000 GHz, and *TCF* of −70 ppm/°C [3]. To improve the microwave dielectric properties of $Mg_4Nb_2O_9$ ceramics, divalent and/or pentavalent substitute cations, such as Ni^{2+}, Co^{2+}, Zn^{2+}, and Mn^{2+} for the Mg^{2+}-sites and/or Ta^{5+}, Sb^{5+}, and V^{5+} for the Nb^{5+}-sites, respectively. [5–9]. In addition, to achieve thermal stability for dielectric ceramic materials and systems to which they are applied, the *TCF* and sintering temperature have been controlled by the addition of B_2O_3, LiF, and $CaTiO_3$ [10–12]. To date, the effects of isovalent substitution on the microwave dielectric properties of $Mg_4Nb_2O_9$ ceramics have not been reported.

In this study, the dependence of the microwave dielectric properties of $Mg_4Nb_2O_9$ ceramics on the isovalent substitution of $(Li^{1+}_{1/5}W^{6+}_{4/5})^{5+}$, $(Mg^{2+}_{1/4}W^{6+}_{3/4})^{5+}$, $(Al^{3+}_{1/3}W^{6+}_{2/3})^{5+}$, and $(Ti^{4+}_{1/2}W^{6+}_{1/2})^{5+}$ at the Nb^{5+}-sites was investigated. Typically, the microwave dielectric properties of $Mg_4Nb_{1.95}(B_xW_{1-x})_{0.05}O_9$ ceramics (B = Li^{1+}, Mg^{2+}, Al^{3+}, Ti^{4+}) have been investigated based on the structural characteristics, such as $Mg_4Nb_{1.95}(Li_{1/5}W_{4/5})_{0.05}O_9$ (MNLW), $Mg_4Nb_{1.95}(Mg_{1/4}W_{3/4})_{0.05}O_9$ (MNMW), $Mg_4Nb_{1.95}(Al_{1/3}W_{2/3})_{0.05}O_9$ (MNAW) and $Mg_4Nb_{1.95}(Ti_{1/2}W_{1/2})_{0.05}O_9$ (MNTW).

* Corresponding author.
E-mail address: eskim@kyonggi.ac.kr (E.S. Kim).

http://dx.doi.org/10.1016/j.ceramint.2017.05.316

2. Experimental procedures

High-purity oxide powders (MgO, Nb_2O_5, Al_2O_3, TiO_2 (99.9%), Li_2CO_3, and WO_3(99%)) were used as raw materials. These powders were batched according to their compositions, e.g., $Mg_4Nb_{1.95}(B_xW_{1-x})_{0.05}O_9$, where B = $(Li^{1+}{}_{1/5}W^{6+}{}_{4/5})^{5+}$, $(Mg^{2+}{}_{1/4}W^{6+}{}_{3/4})^{5+}$, $(Al^{3+}{}_{1/3}W^{6+}{}_{2/3})^{5+}$, and $(Ti^{4+}{}_{1/2}W^{6+}{}_{1/2})^{5+}$. The compounds were ball-milled with ethanol for 24 h in zirconia balls. After calcinations at 1100 °C for 3 h, the calcined powders were milled again for 24 h. Then, the dried powders were pressed isostatically into 10-mm diameter disks at 1500 kg/cm^2. These pellets were sintered at 1350 °C for 10 h in air, and then cooled to room temperature in the furnace.

The crystal structures and phases of the sintered specimens were identified by X-ray powder diffraction analysis (XRD, D/Max-3C, Rigaku, Japan) over a 2θ range of 10–60°. The structural characteristics such as atomic position, lattice parameters, unit-cell volumes, and theoretical densities of the specimens were calculated by Rietveld refinement of the powder XRD patterns using Fullprof (WinPLOTR) [13]. The apparent densities of the samples were measured using the Archimedes method. The relative densities were obtained from the apparent density and the theoretical density. The temperature coefficient of resonant frequency (*TCF*) of the specimens was determined using the cavity method at temperatures ranging from 25 to 80 °C [14]. The dielectric constant (*K*) and quality factor (*Qf*) of samples were measured by Hakki and Coleman's method with a TE_{011} mode at 9.5–10 GHz [15] using a network analyzer.

3. Results and discussion

As shown in Fig. 1, the XRD patterns of the specimens sintered in air at 1350 °C for 10 h in air showed the single phase of corundum with hexagonal symmetry (No. 165, *P*-3*c*1) over the whole range of compositions studied. From the XRD data of the $Mg_4Nb_2O_9$-based ceramics, including the structural characteristics such as the lattice parameters, unit-cell volumes, and theoretical densities calculated by Rietveld refinements, are summarised in Table 1. The R_f factors ranged from 1.46 to 2.77, and the Bragg *R*-factor (R_{Bragg}) was obtained in the range from 1.93 to 2.92, implying that the quality of the Rietveld refinements was excellent, as shown in Fig. 2.

Fig. 3 shows the relationship between the observed dielectric constant ($K_{obs.}$) and the theoretical dielectric constant ($K_{theo.}$) of the specimens substituted with $(Li^{1+}{}_{1/5}W^{6+}{}_{4/5})^{5+}$, $(Mg^{2+}{}_{1/4}W^{6+}{}_{3/4})^{5+}$, $(Al^{3+}{}_{1/3}W^{6+}{}_{2/3})^{5+}$, and $(Ti^{4+}{}_{1/2}W^{6+}{}_{1/2})^{5+}$ at the Nb^{5+}-sites of the $Mg_4Nb_2O_9$-based ceramics. According to Shannon *et al.*, the theoretical

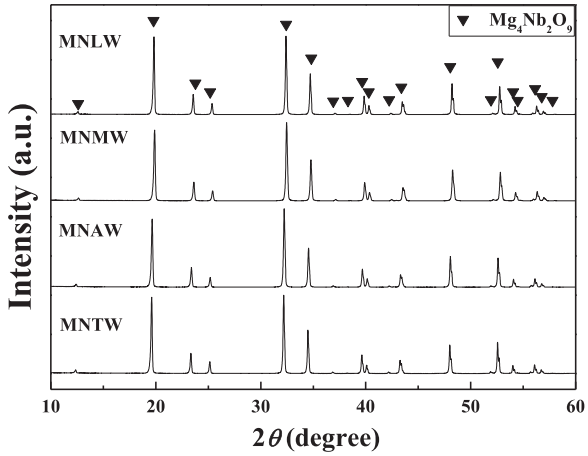

Fig. 1. X-ray diffraction patterns of the $Mg_4Nb_{1.95}(B_xW_{1-x})_{0.05}O_9$ (B = Li, Mg, Al, Ti) ceramics sintered at 1350 °C for 10 h.

ionic polarizability (α_{theo}) and observed dielectric polarizability (α_{obs}) can be calculated using Eqs. (1)–(2) [16]:

$$\alpha_{theo}[Mg_4Nb_{1.95}(B_xW_{1-x})_{0.05}O_9] = 4\alpha_{Mg^{2+}}+1.\ 95\alpha_{Nb^{5+}}+0.\ 05(x)\alpha_B + 0.\ 05(1-x)\alpha_{W^{6+}} + 9\alpha_{O^{2-}}, \quad (1)$$

$$\alpha_{obs} = \frac{1}{4/3\pi}\left[(V_m)\frac{(K-1)}{(K+2)}\right], \quad (2)$$

where the α_i is the ionic polarizability of the species (Mg^{2+}, Nb^{5+}, B (B = Li^{1+}, Mg^{2+}, Al^{3+}, Ti^{4+}), W^{6+}, and O^{2-}). The results of these calculations are listed in Table 2. The K_{theo} of $Mg_4Nb_{1.95}(B_xW_{1-x})_{0.05}O_9$ was calculated by the Clausius-Mosotti Eq. (3):

$$K_{theo} = \frac{3V_m+8\pi\alpha_{theo}}{3V_m-4\pi\alpha_{theo}}, \quad (3)$$

where the V_m is the molar volume. Although the ionic polarizabilities of $(Li^{1+}{}_{1/5}W^{6+}{}_{4/5})^{5+}$ (2.8 Å^3), $(Mg^{2+}{}_{1/4}W^{6+}{}_{3/4})^{5+}$ (2.73 Å^3), $(Al^{3+}{}_{1/3}W^{6+}{}_{2/3})^{5+}$ (2.39 Å^3), and $(Ti^{4+}{}_{1/2}W^{6+}{}_{1/2})^{5+}$ (3.07 Å^3) are all different [16], neither the ionic polarizabilities (α_{obs}, α_{theo}) nor the dielectric constants (K_{obs}, K_{theo}) changed significantly with the type of substituted ion.

Generally, the quality factor (*Qf*) is affected by the density, secondary phase, and porosity [6] of the ceramic material. However, all of the specimens showed single phase of corundum structure with hexagonal symmetry. Because the densities of the samples were nearly full density, the relative densities of the samples are greater than 98% of their theoretical values. Consequently, the effects of the density and secondary phases on the *Qf* value can be neglected [17], as shown in Fig. 1 and Table 2. Finally, the *Qf* value was mainly dependent on the structural characteristics such as the bond valence of the crystal structure. The $Mg_4Nb_2O_9$ ceramics consists of three types of oxygen octahedral: $Mg(1)O_6$, $Mg(2)O_6$, and NbO_6. The NbO_6 octahedra are linked by face sharing, while $Mg(1)O_6$ and $Mg(2)O_6$ octahedra are connected by face sharing, and the other oxygen octahedra are linked by edge and corner sharing [18].

To evaluate the structural characteristics, the bond valence (V_i) between the cations and oxygen ions of the specimens were calculated using Eqs. (4)–(5) [19,20]:

$$v_{i-O} = \exp\left[\frac{R_{i-O} - d_{i-O}}{b}\right], \quad (4)$$

$$V_i = \sum v_{i-O}, \quad (5)$$

where $R_{i\text{-}O}$ is the empirically determined bond valence parameter, *b* is a generally used to be a universal constant (0.37 Å), and $d_{i\text{-}O}$ is the bond length between the cation (*i*) and oxygen ion obtained by Rietveld refinement. The bond valences were calculated from Eqs. (4) and (5), and these are listed in Table 3. According to previous reports [21,22], the bond valence is closely related to the bond strength. High bond strength implies a lower lattice anharmonicity and damping constant of the microwave signal, resulting in a higher *Qf* value. Therefore, the *Qf* values of specimens depended on the bond valence.

Fig. 4 shows the dependence of the *Qf* values on the average bond valence of the specimens sintered at 1350 °C for 10 h. The *Qf* value of specimens with MNTW samples was the highest value (233,000 GHz), arising from its high bond valence compared to those of the other samples.

In general, the negative *TCF* values of the samples were affected by the additives with positive *TCF* values, such as $CaTiO_3$ (+800 ppm/°C) and $SrTiO_3$ (+1600 ppm/°C) ceramics [11,23]. However, as the additive content increased, the *Qf* value of specimens rapidly decreased because of the structural mismatch between the matrix composition and the additives [4]. Therefore, the dependence of the *TCF* value on the structural characteristics must be investigated to improve the *TCF* value of the specimens.

The *TCF* value of the specimens sintered at 1350 °C for 10 h was

Table 1
Reliabilities, lattice parameters, unit-cell volumes, and theoretical densities of the $Mg_4Nb_2O_9$-based ceramics.

Compositions	Reliabilities		Lattice parameter (Å) *a*, *b*, *c*	$V_{unit\text{-}cell}$ (Å^3)	Theoretical density (g/cm^3)
	R_f	R_{Bragg}			
MNLW	1.64	1.93	5.1594, 5.1594, 14.0240	323.300	4.415
MNMW	2.18	2.07	5.1602, 5.1602, 14.0260	323.439	4.411
MNAW	1.46	1.98	5.1562, 5.1562, 14.0185	322.767	4.414
MNTW	2.77	2.92	5.1569, 5.1569, 14.0133	322.731	4.406

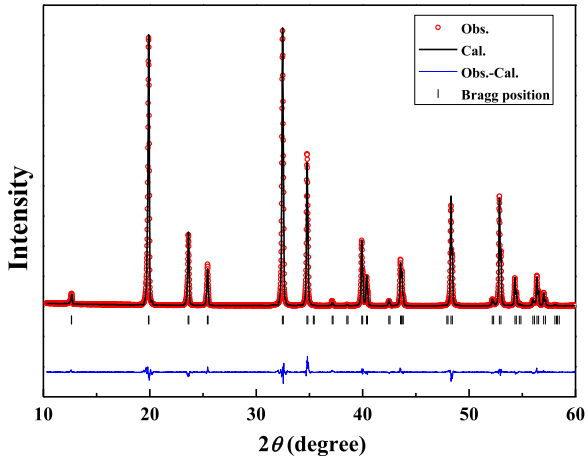

Fig. 2. Rietveld refinement patterns of the $Mg_4Nb_{1.95}(Ti_{1/2}W_{1/2})_{0.05}O_9$ samples sintered at 1350 °C for 10 h.

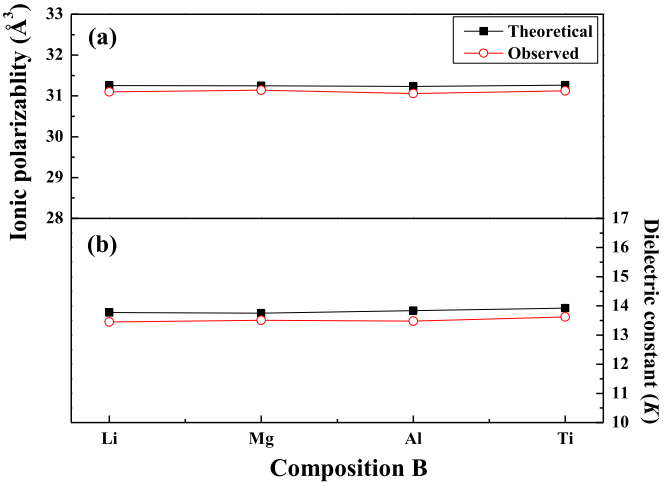

Fig. 3. (a) Theoretical polarizabilities (α_{theo}) and observed polarizabilities (α_{obs}), and (b) theoretical dielectric constants (K_{theo}), and observed dielectric constants (K_{obs}) of the $Mg_4Nb_{1.95}(B_xW_{1-x})_{0.05}O_9$ (B = Li, Mg, Al, Ti) ceramics sintered at 1350 °C for 10 h.

Table 2
Physical properties of $Mg_4Nb_2O_9$-based ceramics sintered at 1350 °C for 10 h.

Compositions	Apparent density (g/cm^3)	Relative density (%)	V_m (Å^3)	α_{theo} (Å)	α_{obs} (Å)
MNLW	4.356	98.6	161.650	31.251	31.098
MNMW	4.356	98.7	161.715	31.248	31.139
MNAW	4.351	98.5	161.384	31.231	31.061
MNTW	4.348	98.6	161.366	31.264	31.124

Table 3
Bond valences and octahedral distortions in the $Mg_4Nb_2O_9$-based ceramics sintered at 1350 °C for 10 h.

Compositions	Bond valence			
	$Mg_{(1)}O_6$	$Mg_{(2)}O_6$	NbO_6	Average
MNLW	2.0086	1.9626	5.0451	3.0054
MNMW	2.0086	2.0662	4.8362	2.9703
MNAW	2.0353	2.1008	4.8858	3.0073
MNTW	2.0284	1.9588	5.4138	3.1337
Compositions	**Octahedral distortion (× 10^3)**			
	$Mg_{(1)}O_6$	$Mg_{(2)}O_6$	NbO_6	Average
MNLW	0.9402	1.6703	2.5199	1.1701
MNMW	0.5220	1.9631	2.9334	1.8061
MNAW	0.1663	2.5096	3.2093	1.9617
MNTW	3.4930	1.9679	4.4045	3.2884

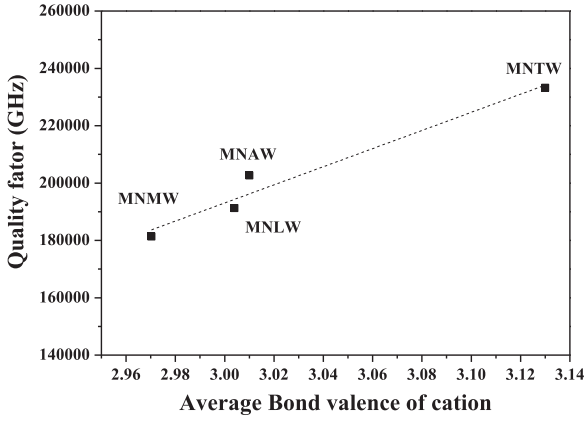

Fig. 4. Relationship between the *Qf* value and the average bond valence of the $Mg_4Nb_{1.95}(B_xW_{1-x})_{0.05}O_9$ (B = Li, Mg, Al, Ti) ceramics sintered at 1350 °C for 10 h.

dependent on the average distortion (Δ_{avg}) of three types of oxygen octahedra ($Mg(1)O_6$, $Mg(2)O_6$, and NbO_6). The octahedral distortion can be calculated using Eq. (6), as reported by Shannon [24]:

$$\Delta = \left(\frac{1}{6}\right) \times \sum \left[\frac{R_i - \overline{R}}{\overline{R}}\right], \quad (6)$$

where R_i and $\overline{R}$ are the individual bond lengths and the average bond length in the oxygen octahedral, respectively. The octahedral distortions in $Mg(1)O_6$, $Mg(2)O_6$, and NbO_6 are shown in Table 3. As the average octahedral distortion increased, the *TCF* values decreased, eventually becoming negative; this agrees well with a previous report for the $(1\text{-}x)Ca_{0.85}Nd_{0.1}TiO_{3-x}LnAlO_3$ system [25], as shown in Fig. 5. These results demonstrate a similar trend to that of the ilmenite structure. The ilmenite structure is an ordered derivative of the corundum structure, and according to Jo *et al.* [26], the *TCF* value is affected by the distortion of oxygen octahedra due to the increase of thermal energy in the ilmenite structure In addition, the increase of thermal energy with temperature would completely absorb to recover the distorted octahedral rather than in recovering the relationship between the polarizability and temperature. These results were affected by the higher average oxygen octahedral distortion (Δ_{avg}) of specimens

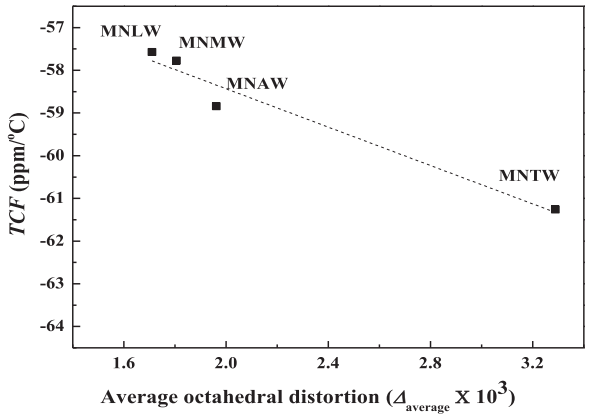

Fig. 5. Dependence of *TCF* value on the average octahedral distortion of $Mg_4Nb_{1.95}(B_xW_{1-x})_{0.05}O_9$ (B = Li, Mg, Al, Ti) ceramics sintered at 1350 °C for 10 h.

with MNTW, arising from the high bond strength of the corundum structure.

4. Conclusions

The microwave dielectric properties of $Mg_4Nb_{1.95}(B_xW_{1-x})_{0.05}O_9$ ceramics (B = Li^{1+}, Mg^{2+}, Al^{3+}, Ti^{4+}) sintered at 1350 °C for 10 h were investigated. The structures were confirmed to be single-phase corundum structures for the whole range of compositions. The *K* values of the samples were similar, and the ionic polarizabilities (α_{obs}, α_{theo}) and dielectric constants (K_{obs}, K_{theo}) of the samples did not vary significantly with different substitution ions. The *Qf* values were affected significantly by the average bond valence of the three types of oxygen octahedra. The $Mg_4Nb_{1.95}(Ti_{1/2}W_{1/2})_{0.05}O_9$ sample showed the highest *Qf* value than other compositions. These results could be attributed to the decrease in the anharmonicity and damping constant associated with the increasing average bond valence. As the average octahedral distortion increased, the *TCF* value decreased, and eventually become negative; the reduction in *TCF* occurred because the increasing thermal energy with temperature was led to recover the distorted octahedra in the corundum structure.

Conflict of interest

We declare that we do not have any commercial or associative interest that represents a conflict of interest in connection with the work submitted.

Acknowledgements

This work was supported by Kyonggi University's Graduate Research Assistantship 2016 and Basic Science Research Program through the National Research Foundation of Korea (NRF) funded by the Ministry of Education, Science, and Technology (2015R1D1A1A09061528).

References

[1] R.J. Cava, Dielectric materials for applications in microwave communications, J. Mater. Chem. 11 (2001) 54–62.
[2] A. Kan, H. Ogawa, Low-temperature synthesis, and microwave dielectric properties of $Mg_4Nb_2O_9$ ceramics synthesized by a precipitation method, J. Alloy. Compd. 364 (2004) (249–249).
[3] A. Kan, H. Ogawa, A. Yokoi, Y. Nakamura, Crystal structural refinement of corundum-structured $A_4M_2O_9$(A = Co and Mg, M = Nb and Ta) microwave dielectric ceramics by high-temperature X-ray powder diffraction, J. Eur. Ceram. Soc. 27 (2007) 2977–2981.
[4] H.J. Jo, E.S. Kim, Enhanced quality factor of $MgTiO_3$ ceramics by isovalent Ti-site substitution, Ceram. Int. 42 (2016) 5479–5486.
[5] B.J. Li, S.Y. Wang, Y.B. Chen, Dielectric properties and crystal structure of $(Mg_{0.95}Ni_{0.05})_4(Nb_{1-x}Ta_x)_2O_9$, J. Mater. Sci. Eng. 3 (2) (2014) 140.
[6] Y.B. Chen, Dielectric properties and crystal structure of $Mg_4Nb_2O_9$ ceramics with Mg^{2+} substituted by Zn^{2+} and Co^{2+}, Jpn. J. Appl. Phys. 51 (2012) 085804.
[7] A. Kan, H. Ogawa, Microwave dielectric properties of corundum-structured $(Mg_{4-x}M_x)(Nb_{2-y}A_y)O_9$ (M = Mn, Co, and Zn; A = Ta, and Sb) ceramics, in: Proceedings of the 2017 Sixteenth IEEE International Symposium on the Applications of Ferroelectrics, IEEE, 2007, pp. 519–522.
[8] H. Ogawa, H. Taketani, A. Kan, A. Fujita, G. Zouganelis, Evaluation of electronic state of $Mg_4(Nb_{2-x}Sb_x)O_9$ microwave dielectric ceramics by first principle calculation method, J. Eur. Ceram. Soc. 25 (2005) 2859–2863.
[9] A. Kan, H. Ogawa, A. Yokoi, H. Osato, Low-temperature sintering and microstructure of $Mg_4(Nb_{2-x}V_x)O_9$ microwave dielectric ceramic by V substitution for Nb, Jpn. J. Appl. Phys. 42 (2003) 6154–6157.
[10] H.T. Wu, L.X. Li, B_2O_3 additives on sintering and microwave dielectric behaviors of $Mg_4Nb_2O_9$ ceramics synthesized through the aqueous sol–gel process, J. Sol.-Gel Sci. Technol. 58 (1) (2011) 48–55.
[11] G. Yao, P. Liu, Low-temperature sintering and microwave dielectric properties of $(1-x)Mg_4Nb_2O_9$-$xCaTiO_3$ ceramics, Physica B 405 (2010) 547–551.
[12] A. Yokoi, H. Ogawa, A. Kan, H. Osato, Y. Higashida, Microwave dielectric properties of $Mg_4Nb_2O_9$-3.0 wt% LiF ceramics, J. Eur. Ceram. Soc. 25 (2005) 2871–2875.
[13] T. Roisnel, J.R. Carvajal, WinPLOTR: a windows tool for powder diffraction pattern analysis, Mater. Sci. Forum 378–381 (2001) 118–123.
[14] T. Nishikawa, K. Wakino, H. Tamura, H. Tanaka, Y. Ishikawa, Precise measurement method for temperature coefficient of microwaved dielectric resonator material, in: Microwave Symposium Digest, vol. 87, 1987, pp. 277–280.
[15] C.B.W. Hakki, P.D. Coleman, A dielectric resonator method of measuring inductive capacities in the millimeter range, Microw. Theory Tech. 8 (1960) 402–410.
[16] R.D. Shannon, Dielectric polarizabilities of ions in oxides and fluorides, J. Appl. Phys. 73 (1993) 348–366.
[17] D.M. Iddles, A.J. Bell, A.J. Moulson, Between dopants, microstructure and the microwave dielectric properties of ZrO_2-TiO_2-SnO_2 ceramics, J. Mat. Sci. 27 (1992) 6303–6310.
[18] Y.C. You, H.L. Park, Y.G. Song, H.S. Moon, G.C. Kim, Stable phases in the MgO-Nb_2O_5 system at 1250 °C, J. Mater. Sci. Lett. 13 (1994) 1487–1489.
[19] I.D. Brown, D. Altermatt, Bond-valence parameters obtained from a systematic analysis of the inorganic crystal structure database, Acta Crystallogr. B 41 (1985) 244–247.
[20] I.D. Brown, K.U. Kang, Empirical parameters for calculating cation-oxygen bond valences, Acta Crystallogr. B 32 (1976) 1957–1959.
[21] J. Li, Y. Han, T. Qiu, C. Jin, Effect of bond valence on microwave dielectric properties of $(1-x)CaTiO_3$–$x(Li_{0.5}La_{0.5})TiO_3$ ceramics, Mater. Res. Bull. 47 (2012) 2375–2379.
[22] S.K. Singh, V.R.K. Murthy, Crystal structure, Raman spectroscopy and microwave dielectric properties of layered-perovskite BaA2Ti3O10 (A = La, Nd and Sm) compounds, Mater. Chem. Phys. 160 (2015) 187–193.
[23] G. Yao, P. Iu, H. Ma, X. Tian, The sintering behavior and microwave dielectric properties of $Mg_4Nb_2O_9$/$SrTiO_3$ composite ceramic, Chin. J. Mater. Res. 24 (4) (2010) 444–448.
[24] R.D. Shannon, Revised effective ionic radii and systematic studies of interatomic distances in halides and chalcogenides, Acta Crystallogr. A 32 (5) (1976) 751–767.
[25] E.S. Kim, B.S. Chun, D.H. Kang, Effects of structural characteristics on microwave dielectric properties of $(1-x)Ca_{0.85}Nd_{0.1}TiO_{3-x}LnAlO_3$ (Ln = Sm, Er and Dy) ceramics, J. Eur. Ceram. Soc. 27 (8–9) (2007) 3005–3010.
[26] E.S. Kim, K.H. Yoon, Microwave dielectric properties of $(1-x)CaTiO_3$-$xLi_{1/2}Sm_{1/2}TiO_3$ ceramics, J. Eur. Ceram. Soc. 23 (2003) 2397–2401.